Eur J Med Chem (1993) 28, 149–158

Synthesis, crystal structure and biological properties of a new series of lipophilic *s*-triazines, dihydrofolate reductase inhibitors

P Tsitsa[1], E Antoniadou-Vyza[1]*, SJ Hamodrakas[2]**, EE Eliopoulos[3], A Tsantili-Kakoulidou[1], E Lada-Hytiroglou[4], C Roussakis[5], I Chinou[5], A Hempel[6], N Camerman[6], FP Ottensmeyer[2], DA Vanden Berghe[7]

[1]*Department of Pharmaceutical Chemistry, University of Athens, Panepistimiopolis, Athens 157 01;*
[2]*Department of Medical Biophysics, University of Toronto, 500 Sherbourne St, Toronto M4X 1K9;*
[3]*Department of Biochemistry and Molecular Biology, University of Leeds, Leeds LS2 9JT, UK;*
[4]*Department of Microbiology, Faculty of Medicine, University of Athens, Goudi GR-11527, Athens, Greece;*
[5]*Laboratoire de Pharmacognosie et de Biologie Végétale, Université de Nantes, 1, rue Gaston-Veil, BP 1024, 44035 Nantes Cedex 01, France;*
[6]*Department of Biochemistry, University of Toronto, School of Medicine, Toronto, Canada M5S 1A8;*
[7]*Department of Geneeskunde, Universitaire Instelling Antwerpen, Universiteitsplein 1-B-2610, Antwerp, Belgium*

(Received 4 January 1992; accepted 3 August 1992)

Summary — A number of adamantyl-group-bearing diamino-*s*-triazines were synthesized as potential dihydrofolate reductase (DHFR) inhibitors and their pharmacological properties were tested. The crystal structures of certain compounds were determined by X-ray crystallography. With the aid of computer graphics, model structures of the L1210 mouse DHFR–ligand ternary complex were constructed. The binding affinities of the compounds to DHFR were determined experimentally. Compounds mono-substituted at the nitrogen of the amine group appear to be slightly better inhibitors. Weak activity was also enhanced by the presence of a methylene bridge between the adamantyl group and the *s*-triazine ring. The majority of the compounds was shown to have weak activity against P388 and KB cell lines *in vitro*; some compounds showed weak anti-bacterial activity and no anti-viral activity was detected.

dihydrofolate reductase (DHFR) inhibitors / *s*-triazines / adamantyl derivatives / synthesis / crystal structure / biological properties

Introduction

The discovery that diamino-*s*-triazines interfere with folic acid metabolism and show promise in cancer chemotherapy has triggered an enormous amount of research on the anti-folate activity of this class of compounds [1–3]. One of the conclusions drawn from these studies is that, for several anti-folates, the extent of their uptake, their growth inhibitory potency on tumor cells as well as their affinity for dihydrofolate reductase (DHFR) correlates well with lipophilicity [4].

In the course of our investigation on adamantane-ring-bearing compounds [5, 6] we considered the possibility that this group attached to a triazine ring could make advantageous use of the enzyme's hydrophobic cavity. In addition, a paucity of information on amino-substituted analogs, such as antifolates, in contrast to the plethora of similar information available on the diamino-derivatives, prompted us to attempt substitution on the 6-amino nitrogen of the *s*-triazine molecule. Therefore, potential DHFR inhibitors of the general type **1** and **2** (fig 1) were synthesized as possible anti-tumor, anti-bacterial and anti-fungal agents (table I). Additionally, in order to clarify to what extent the activity is influenced by the presence or by the position of the adamantyl moiety, three other compounds were prepared. Compounds **3a, b** bear a *tert*-butyl-phenyl group whose lipophilicity is similar to that of the adamantyl group, while the adamantyl group in compound **4** is attached to the amine nitrogen (fig 1 and table I).

All compounds have been tested for DHFR-binding affinity and pharmacological properties. In order to understand the observed variation in biological ac-

*Correspondence and reprints.
**Present address:* Department of Biology, University of Athens, Athens 157 01, Greece.

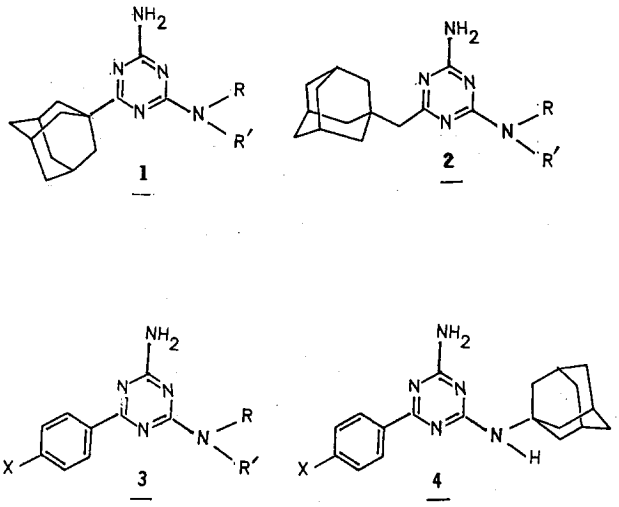

Fig 1. Compounds **1–4**.

Table I. Structure and physical data of the synthesized triazines.

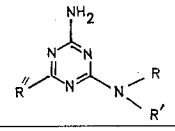

No	R′	-N(R)(R′)	Yield %	Molec.Form.	m.p.(°C) base	m.p.(°C) HCL
a	Ad	-N(CH3)2	58	$C_{15}H_{23}N_5$	230-2[a]	312-3[b]
b	Ad	-N⟨ ⟩	48	$C_{18}H_{27}N_5$	183-5[a]	249-51[d]
c	Ad	-N⟨ O ⟩	60	$C_{17}H_{25}N_5O$	172-4[a]	284-6[d]
d	Ad	-N⟨ N-CH3 ⟩	53	$C_{18}H_{28}N_6$	196-7[a]	278-80[d]
e	Ad	-NH-⟨ ⟩	30	$C_{19}H_{29}N_5$	172-5[b]	192-3[d]
f	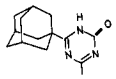			$C_{15}H_{22}N_4O$	110 dec	140 dec
1a	Ad-CH2 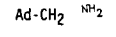	-N(CH3)2	62	$C_{16}H_{25}N_5$	219-20[a]	274-6[d]
1b	Ad-CH2	-NH-⟨ ⟩	56	$C_{20}H_{31}N_5$	179-90[a]	198-9[d]
1a	t-Bu-⟨ ⟩-CH2	-NHCH2-⟨ ⟩	40	$C_{22}H_{15}N_5$	138-40[a]	217-8[d]
1b	t-Bu-⟨ ⟩-CH2	-NH-⟨ ⟩	18	$C_{21}H_{29}N_5$	154-6[a]	222-4[d]
	⟨ ⟩-CH2	-NH- 	25	$C_{20}H_{25}N_5$	195-7[c]	>300[c]

Ad: adamantyl. [a]Free base recrystallized from MeCN. [b]Recrystallized from MeOH. [c]Recrystallized from EtOH. [d]Recrystallized from Et_2O.

tivity and compare structure and binding with other anti-folate ligands [7, 8], crystal structure determinations and conformational analyses of both active and inactive lipophilic compounds were carried out. Modeling studies of L1210 mouse DHFR–ligand ternary complexes were also performed using an interactive graphics system.

Chemistry

The preparation of the biguanide hydrochlorides **5** (scheme 1) was effected by fusion of equimolecular mixtures of mono- or disubstituted amine hydrochlorides and dicyanediamide. The reaction temperature was maintained at 130–150°C for several hours and the products were isolated as hydrochloric salts [9, 10]. Compounds shown in table I were synthesized according to Guioca [11] from the biguanides **5** and the appropriate esters **6**, **7** in the presence of sodium methoxide. The reaction is an acylation followed by cyclization. The whole reaction is presented in scheme 1.

It is well known that similar compounds exhibit thermal stability problems and that they are base labile [12]. They are sensitive to solvolysis not only in water but also in alcohols and other solvents bearing hydroxyl groups. Thus, 1,3,5-triazin-6(5*H*)-on **1f** (table I), was obtained as a by-product of the synthesis of **1a**, when we were trying to optimize the yield by heating the reaction mixture at a higher temperature for a longer period of time. After separation and purification, structure identification became possible by IR and NMR spectroscopies, as well as by elemental analysis.

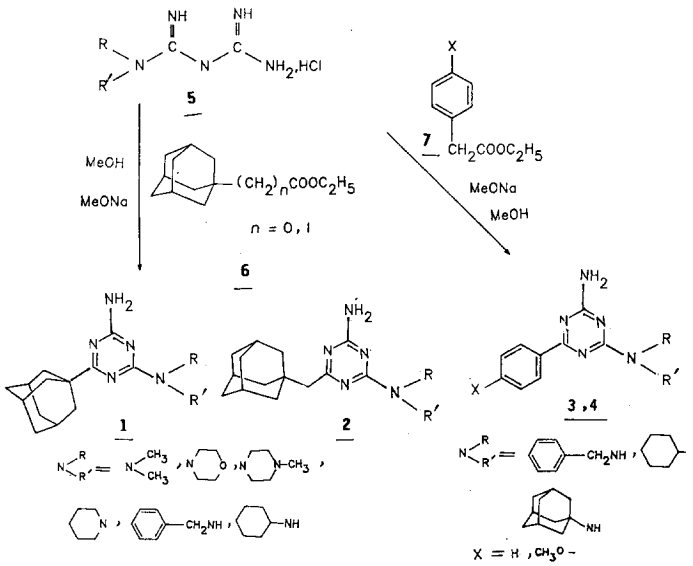

Scheme 1.

X-ray crystallographic studies

Most compounds listed in table I have been crystallized and several crystal structures have been determined by X-ray crystallography (**1a**, **1c**, **1d**, **1e**, **2a**). The crystal structures of **1a**, **1d**, **2a** will be reported elsewhere [13, 14]. Here, we present the structures of **1c** and **1e**.

Bond lengths and angles and torsion angles of **1c** and **1e** are listed in tables II and III, respectively. Figure 2 shows perspective views of the molecules and the atomic numbering scheme used.

Table II. Bond lengths and angles and torsion angles of **1c**, with estimated standard deviations in parentheses.

Bond lengths (Å)		*Bond angles (deg)*	
N(1) –C(2)	= 1.30(2)	C(6) –N(1) –C(2)	= 116(2)
C(2) –N(3)	= 1.37(2)	N(1) –C(2) –N(3)	= 127(2)
C(2) –N(7)	= 1.35(2)	N(1) –C(2) –N(7)	= 117(2)
N(3) –C(4)	= 1.37(2)	N(7) –C(2) –N(3)	= 117(2)
C(4) –N(5)	= 1.30(3)	C(2) –N(3) –C(4)	= 114(2)
N(5) –C(6)	= 1.39(2)	N(3) –C(4) –N(5)	= 124(2)
C(6) –N(1)	= 1.35(3)	N(3) –C(4) –C(9)	= 118(2)
C(6) –N(8)	= 1.33(3)	C(9) –C(4) –N(5)	= 118(2)
N(8) –C(19)	= 1.48(3)	C(4) –N(5) –C(6)	= 117(2)
C(19)–C(20)	= 1.54(3)	N(5) –C(6) –N(1)	= 123(2)
C(20)–O(21)	= 1.46(3)	N(5) –C(6) –N(8)	= 117(2)
C(21)–C(22)	= 1.39(3)	N(8) –C(6) –N(1)	= 120(2)
C(22)–C(23)	= 1.49(3)	C(6) –N(8) –C(19)	= 120(2)
C(23)–N(8)	= 1.44(3)	N(8) –C(19)–C(20)	= 109(2)
C(4) –C(9)	= 1.44(3)	C(23)–N(8) –C(6)	= 127(2)
C(9) –C(10)	= 1.56(3)	C(19)–C(20)–O(21)	= 109(2)
C(9) –C(11)	= 1.57(3)	C(20)–O(21)–C(22)	= 111(2)
C(9) –C(12)	= 1.60(3)	O(21)–C(22)–C(23)	= 111(2)
C(10)–C(13)	= 1.52(3)	C(22)–C(23)–N(8)	= 111(2)
C(11)–C(15)	= 1.54(3)	C(23)–N(8) –C(19)	= 113(2)
C(12)–C(17)	= 1.55(3)	C(4) –C(9) –C(10)	= 108(2)
C(13)–C(14)	= 1.51(3)	C(4) –C(9) –C(11)	= 116(2)
C(14)–C(15)	= 1.50(3)	C(4) –C(9) –C(12)	= 111(2)
C(15)–C(16)	= 1.56(3)	C(10)–C(9) –C(11)	= 109(2)
C(16)–C(17)	= 1.51(3)	C(10)–C(9) –C(12)	= 109(2)
C(17)–C(18)	= 1.41(3)	C(11)–C(9) –C(12)	= 104(2)
C(13)–C(18)	= 1.59(3)	C(9) –C(10)–C(13)	= 110(2)
		C(9) –C(11)–C(15)	= 113(2)
		C(9) –C(12)–C(17)	= 109(2)
		C(10)–C(13)–C(14)	= 111(2)
		C(10)–C(13)–C(18)	= 106(2)
		C(13)–C(14)–C(15)	= 112(2)
		C(14)–C(15)–C(16)	= 110(2)
Torsion angles (deg)		C(11)–C(15)–C(14)	= 108(2)
		C(11)–C(15)–C(16)	= 106(2)
N(3)–C(4)–C(9)–C(11)	= 1(2)	C(15)–C(16)–C(17)	= 110(2)
N(3)–C(4)–C(9)–C(10)	= –121(2)	C(12)–C(17)–C(16)	= 106(2)
N(3)–C(4)–C(9)–C(12)	= 120(2)	C(16)–C(17)–C(18)	= 117(2)
N(1)–C(6)–N(8)–C(19)	= 4(2)	C(12)–C(17)–C(18)	= 112(2)
N(1)–C(6)–N(8)–C(23)	= 177(2)	C(13)–C(18)–C(17)	= 109(2)

Contrary to the pyrimidine analogs with the lipophilic substitution at position 5 of the pyrimidine ring that disrupts the ring planarity [7, 8], in these triazines with the adamantyl substitution at position 4 no such effect is observed. The maximum deviation from the plane of the triazine is 0.2 Å.

It is interesting to note that only two orientations of the adamantyl moiety relative to the triazine ring are observed in the solved crystal structures: one has a C–C bond of the adamantyl moiety in a somewhat eclipsed conformation relative to N(3)–C(4) of the triazine ring (**1c**, torsion angle N(3)–C(4)–C(9)–C(11)

Table III. Bond lengths and angles and torsion angles of **1e**, with estimated standard deviations in parentheses.

Bond lengths (Å)		*Bond angles (deg)*	
N(1) –C(2)	= 1.37(3)	C(6) –N(1) –C(2)	= 114(2)
C(2) –N(3)	= 1.37(2)	N(1) –C(2) –N(3)	= 125(2)
C(2) –N(7)	= 1.36(2)	N(1) –C(2) –N(7)	= 116(2)
N(3) –C(4)	= 1.29(3)	N(7) –C(2) –N(3)	= 118(2)
C(4) –N(5)	= 1.32(3)	C(2) –N(3) –C(4)	= 111(2)
N(5) –C(6)	= 1.36(2)	N(3) –C(4) –N(5)	= 130(2)
C(6) –N(1)	= 1.32(3)	N(3) –C(4) –C(9)	= 114(2)
C(6) –N(8)	= 1.29(3)	C(9) –C(4) –N(5)	= 115(2)
N(8) –C(19)	= 1.43(3)	C(4) –N(5) –C(6)	= 114(2)
C(19)–C(20)	= 1.57(3)	N(5) –C (6) –N(1)	= 125(2)
C(20)–C(21)	= 1.46(3)	N(5) –C(6) –N(8)	= 118(2)
C(21)–C(22)	= 1.45(3)	N(8) –C(6) –N(1)	= 117(2)
C(22)–C(23)	= 1.51(3)	C(6) –N(8) –C(19)	= 126(2)
C(23)–C(24)	= 1.53(2)	N(8) –C(19)–C(20)	= 114(2)
C(24)–C(19)	= 1.52(2)	N(8) –C(19)–C(24)	= 114(2)
C(4) –C(9)	= 1.51(3)	C(20)–C(19)–C(24)	= 107(2)
C(9) –C(10)	= 1.53(2)	C(19)–C(20)–C(21)	= 112(2)
C(9) –C(11)	= 1.58(3)	C(20)–C(21)–C(22)	= 117(2)
C(9) –C(12)	= 1.55(3)	C(21)–C(22)–C(23)	= 111(2)
C(10)–C(13)	= 1.57(3)	C(22)–C(23)–C(24)	= 110(2)
C(11)–C(15)	= 1.52(3)	C(23)–C(24)–C(19)	= 112(2)
C(12)–C(17)	= 1.51(3)	C(4) –C(9) –C(10)	= 111(2)
C(13)–C(14)	= 1.52(3)	C(4) –C(9) –C(11)	= 110(2)
C(14)–C(15)	= 1.54(3)	C(4) –C(9) –C(12)	= 116(2)
C(15)–C(16)	= 1.51(3)	C(10)–C(9) –C(11)	= 106(2)
C(16)–C(17)	= 1.50(3)	C(10)–C(9) –C(12)	= 108(2)
C(17)–C(18)	= 1.56(3)	C(11)–C(9) –C(12)	= 105(2)
C(13)–C(18)	= 1.55(3)	C(9) –C(10)–C(13)	= 114(2)
		C(9) –C(11)–C(15)	= 112(2)
		C(9) –C(12)–C(17)	= 114(2)
		C(10)–C(13)–C(14)	= 106(2)
		C(10)–C(13)–C(18)	= 107(2)
		C(13)–C(14)–C(15)	= 111(2)
Torsion angles (deg)		C(14)–C(15)–C(16)	= 108(2)
		C(11)–C(15)–C(14)	= 107(2)
N(3)–C(4)–C(9) –C(11)	= 62(2)	C(11)–C(15)–C(16)	= 112(2)
N(3)–C(4)–C(9) –C(10)	= –54(2)	C(15)–C(16)–C(17)	= 112(2)
N(3)–C(4)–C(9) –C(12)	= –178(2)	C(12)–C(17)–C(16)	= 113(2)
N(1)–C(6)–N(8) –C(19)	= 5(2)	C(16)–C(17)–C(18)	= 104(2)
C(6)–N(8)–C(19)–C(20)	= –86(2)	C(12)–C(17)–C(18)	= 108(2)
C(6)–N(8)–C(19)–C(24)	= 151(2)	C(13)–C(18)–C(17)	= 111(2)

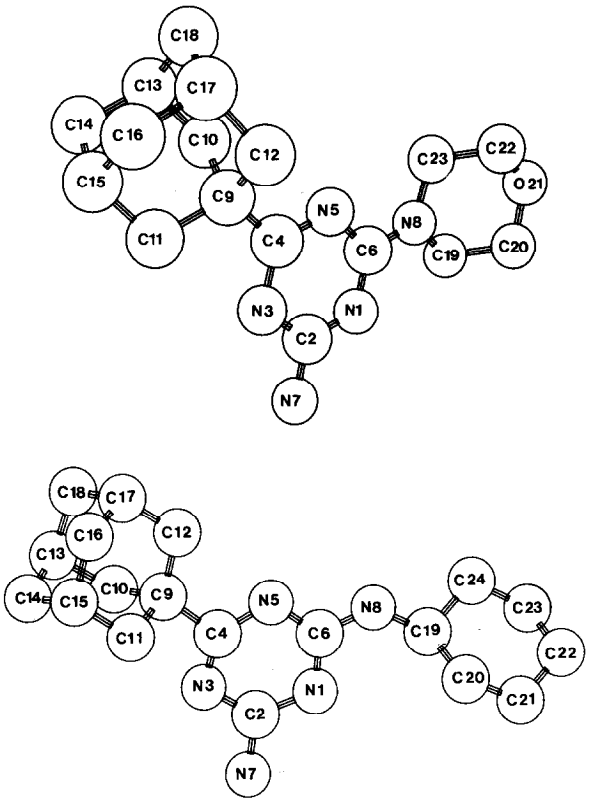

Fig 2. a. A perspective diagram of 2-amino-4-(tricyclo-[3.3.1.1^{3,7}]decyl-1)-6-morpholino-1,3,5-triazine **1c** showing the atomic numbering scheme. The torsion angles shown in table II describe the conformation of the molecule in the crystal. **b.** A perspective diagram of 2-amino-4-(tricyclo[3.3.1.1^{3,7}]decyl-1)-6-cyclohexylamino-1,3,5-triazine **1e** showing the atomic numbering scheme. The torsion angles shown in table III describe the conformation of the molecule in the crystal.

= 1°, table II; **1a**, torsion angle N(3)–C(4)–C(9)–C(11) = –2.4° [14]) and the other a C–C bond of the adamantyl system approaching an eclipsed conformation relative to C(4)–N(5) of the triazine ring (**1e**, torsion angle N(3)–C(4)–C(9)–C(12) = –178°, table III). The two conformations differ by a relative rotation of 60° of the symmetrical adamantyl moiety around the C(4)–C(9) bond that connects adamantyl with the triazine ring. Interestingly, both conformations are observed simultaneously in the crystal structure of **1d** [13], which crystallizes in space group $R\bar{3}$ with two statistically disordered adamantyl positions (torsion angles of 21° and 23° from eclipse for the two orientations). Conformational analysis, using semi-empirical INDO (intermediate neglect of differential overlap) energy calculations, suggests that there is little difference in total molecular energy for rotation about the C(4)–C(9) bond.

The conformation of the substituents at position 6 of the triazine ring (fig 2) is determined by the torsion angle N(1)–C(6)–N(8)–C(19). In all crystal structures solved (tables II and III) [13, 14], this angle is always close to 0°.

The hydrogen-bonding schemes in the crystal structures might reflect patterns existing in the DHFR–ligand complexes. In the crystal structure of **1c**, pairs of molecules related by a center of symmetry (space group P1) are connected by N(3)...N(7) hydrogen bonds (N(3)...N(7) = 3.0 Å). In the crystal structure of **1e**, a similar hydrogen bond connects centrosymmetrically related molecules (N(3)...N(7) = 3.0 Å). Moreover, two methanol molecules per asymmetic unit (space group $P2_1/c$) are also involved in hydrogen bonds; one acts simultaneously as an acceptor to the amino group at position 7 (N(7)) and as a donor to N(1), and the other as an acceptor from the amino group at position 8 (N(8)). The hydrogen bonds observed are rather strong (N...0 distances = 2.8–3.0 Å). In contrast, however, in **1d** hydrogen bonds are observed between N(7) of one molecule and N(21) of the piperazine ring of another molecule [13]. N(3) is not involved, probably due to crystal packing constraints.

Modelling of the L1210 DHFR–ligand ternary complex

The precise molecular geometries of the triazine analogs determined from the X-ray crystallographic studies were used in the modelling studies. Model structures of the compounds were placed in the binding site of DHFR, as determined in the crystal structure of the L1210 mouse DHFR–trimethoprim complex [15], with the triazine ring superimposed on the pyrimidine ring of trimethoprim. Figure 3a–c shows models of the L1210 mouse DHFR–**1c**, –**1d** and –**2b** complexes respectively. In figures 4a and b, several ligands were superimposed in the binding site of the enzyme. Hydrogen bonds may be formed between N(3) and the amino group N(7) of the triazine ring with Glu^{30} of DHFR, and the latter amino group (N(7)) *via* a water molecule to Thr^{136}.

Fig 3. Stereo diagram of the putative model of the L1210 mouse DHFR ternary complex with NADPH and: **1c** of table I (**a**), **1d** of table I (**b**) and **2b** of table I (**c**). Hydrogen bonds described in the text are shown with dashed lines. →

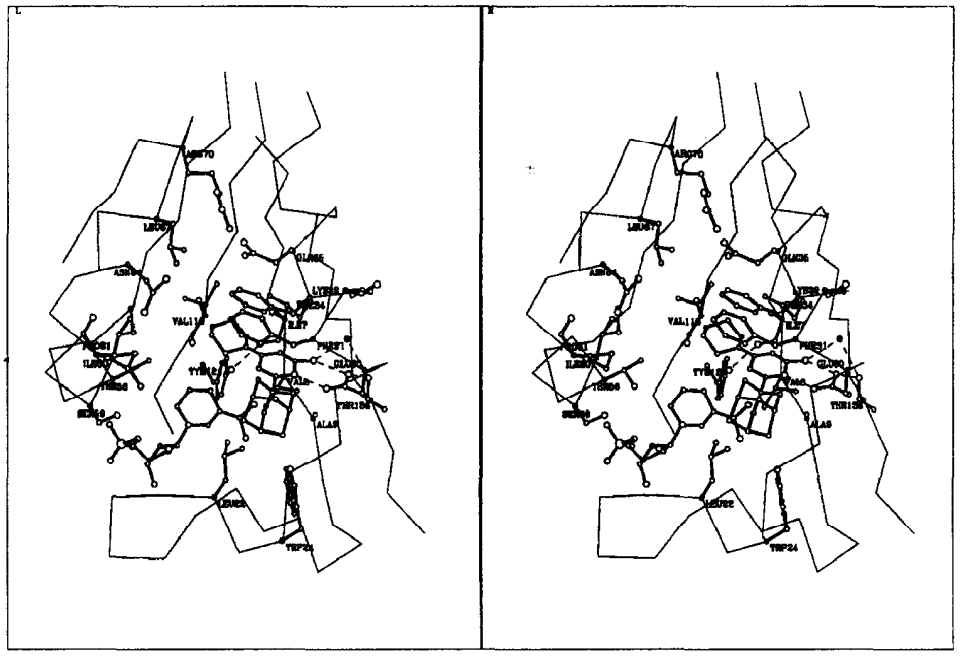

3A

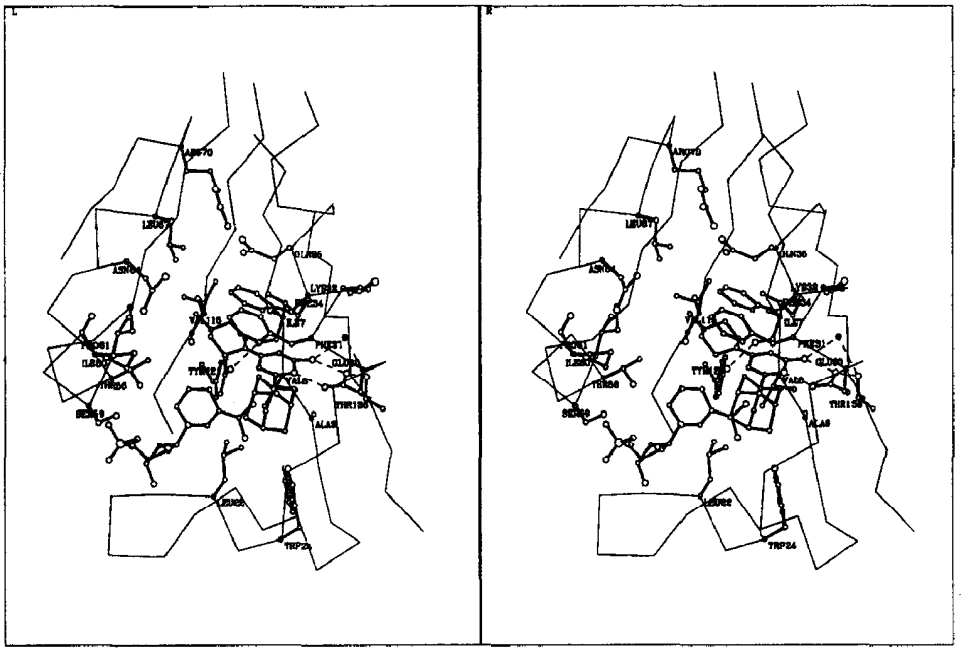

3B

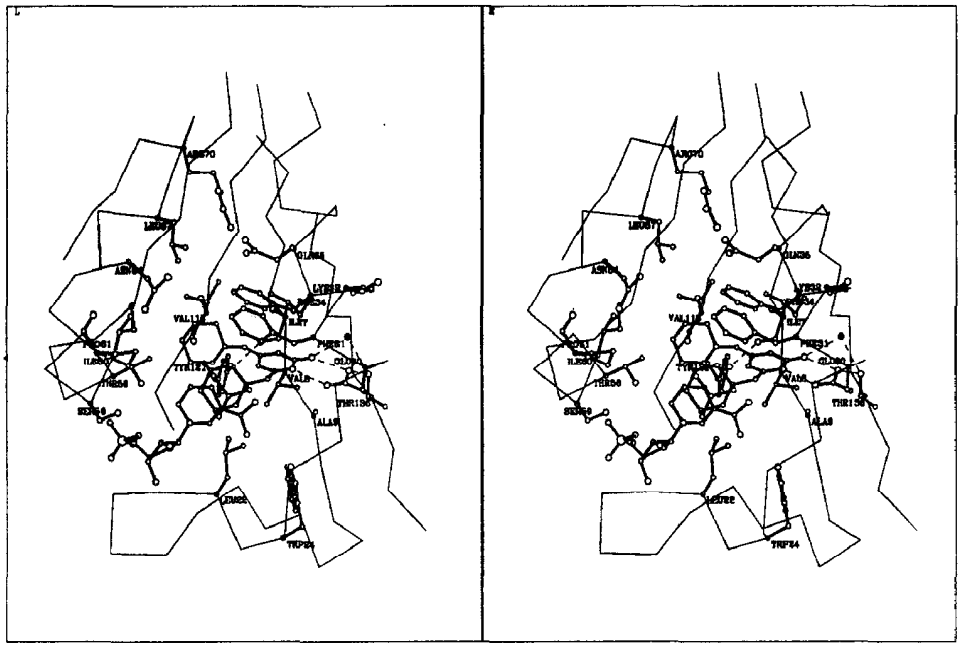

3C

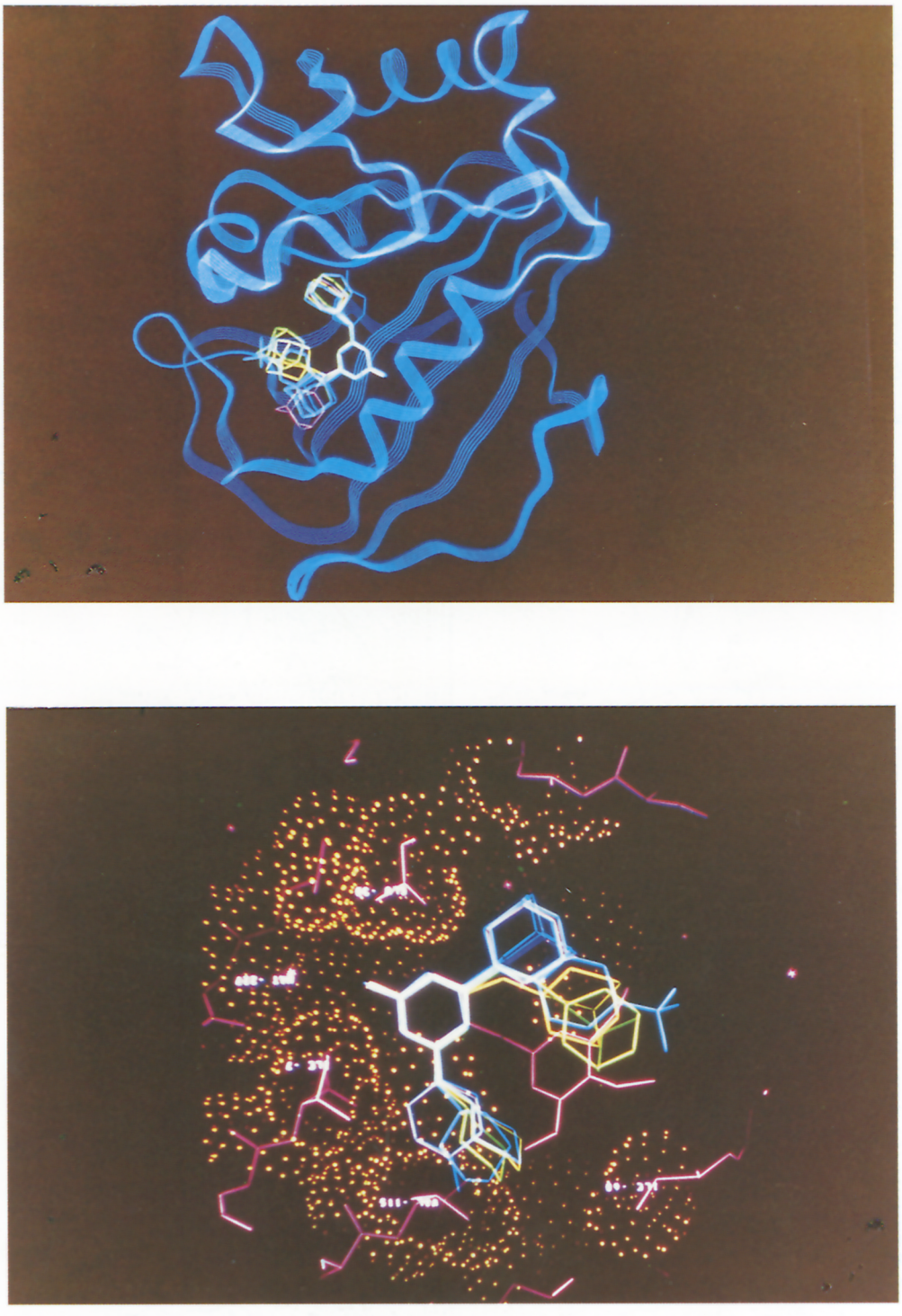

Fig 4. Model structures of L1210 mouse DHFR with the triazine analogs placed in the binding site of the enzyme. The triazine ring of the compounds was superimposed on the pyrimidine ring of trimethoprim [15]. **a.** General view of a ribbon diagram of the enzyme. **b.** The binding site with the van der Waals surface of the protein is displayed in orange.

Biological results

The compounds were tested in various biological assays. They were examined for inhibitory activity against L1210 mouse DHFR [16] and anti-tumor activity against P388 leukemia cells, 9KB5 and NSCLCN6 tumor cells [17–19]. Most compounds were also tested for anti-bacterial, anti-fungal [20, 21] and anti-viral [22] activities *in vitro*. All biological results are summarized in table IV.

Only a weak inhibitory activity against L1210 mouse DHFR was observed. The percentage of inhibition in the presence of 50 μM of each compound was determined (table IV). I_{50} values (concentrations of inhibitor necessary to reduce enzyme activity by 50%) could be established only for **1e**, **2a** and **2b** (these were 80, 112 and 44 μM, respectively), which exhibited the most significant inhibitory activities. The I_{50} value (26.7 μM) and the percentage of inhibition caused by 50 μM of trimethoprim (table IV) were determined under the same conditions.

The majority of the compounds tested exhibited weak activity against human rhinopharynx cancer KB and murine leukemia P388 cell lines *in vitro*. However, all of them were inactive against bronchopulmonary carcinoma (NSCLCN6). It is remarkable to note that only **1a** was inactive on the KB cell line, while still showing some specific activity against P388 cells; the converse occurs more often.

None of the products showed any significant activity against herpes simplex and polio I viruses at non-toxic concentrations on VERO cells, whereas they were toxic at concentrations of 100–200 μg/ml.

Discussion

The existence or lack of a potential hydrogen bond between the amino group at position 6 of the triazine ring and the carbonyl oxygen of Ile[7] is reflected in the binding affinity of the compounds for DHFR, given in table IV. It is evident that compounds **1e**, **2b**, **3b** and **4**, with monosubstitution at the amine nitrogen, are relatively better inhibitors, even if the substituent is as bulky as the adamantyl moiety. This is in agreement with the general requirements for the binding of inhibitors to DHFR from any species [23].

The other major area of interest in the binding to DHFR of this triazine family is the nature of the group at position 4.

In this series of 4-adamantyl *s*-triazines, the presence of a methylene bridge between the lipophilic adamantyl moiety and the *s*-triazine generally increases binding (table IV). This part of the binding site is partly accessible to solvent but, in order to accommodate the volume of the adamantyl group directly linked to the triazine ring, the DHFR structure must be disturbed. The introduction of a methylene

Table IV. Biological data.

No	*% Inh L1210 mouse DHFR*	*ID_{50} KB (μg/ml)*	*ID_{50} P388 (μg/ml)*	*% Growth inhibition*								
				EC[a]	*PM*	*SF*	*SA*	*PsA*	*CA*	*PV*	*AV*	*CC*
1a	18.0	Inac	0.10	10	15	20	0	0	20	20	30	30
1b	18.6	1.00	1.00	–	10	10	20	0	40	25	40	75
1c	6.6	1.00	Inac	10	15	0	–	0	0	50	100	55
1d	12.0	1.00	Inac	10	15	100	100	0	10	65	60	–
1e	29.0	1.00	Inac	10	15	0	20	–	40	50	100	45
1f	31.3	1.00	1.00	–	–	100	100	–	–	–	–	–
2a	32.3	0.99	Inac	0	15	0	26	55	0	70	50	28
2b	49.8	–	–	0	0	0	26	69	0	53	–	5
3a	13.8	1.00	1.00	8	12	8	0	0	–	–	–	–
3b	30.7	1.00	1.00	–	–	–	–	–	–	–	–	–
4	32.2	1.00	Inac	55	50	6	100	0	0	–	–	–
Tr[b]	63.0											
Mico									100	100	100	100
Bp[c]				100	100	100	100	100				

[a]EC: *Escherichia coli*; PM: *Proteus mirabilis*; SF: *Streptococcus faecalis*; SA: *Staphylococcus aureus*; PsA: *Pseudomonas aeruginosa*; CA: *Candida albicans*; PV: *Penicillium verucosum*; AV: *Aspergillus versicolor*; CC: *Cladosporium cladosporoides*. [b]Tr: trimethoprim; Mico: miconazole. [c]Bp: benzylpenicillin. Inac: inactive.

bridge between the adamantyl group and the triazine ring places that group closer to the wider opening of the binding pocket, eliminating the close contact between adamantyl and the side chains of the protein. With this addition of an extra degree of freedom, molecular shapes similar to other adamantyl antifolates may be adopted [7, 8]. This might be related to the relatively high DHFR-inhibitory activities of **2a** and **2b**.

Compound **2b** combines both favorable characteristics, a monosubstituted amine nitrogen and a methylene bridge, and is indeed the most potent analog. For this compound, an I_{50} of 44.0 μM was determined, whereas the I_{50} of trimethoprim under the same conditions is 26.7 μM.

By modifying the adamantyl group of the bridged compounds to *tert*-butyl-phenyl, a slight drop in binding affinity was observed (table IV). This might be due to exposure of this lipophilic group to solvent.

It is interesting to note that 1,3,5 triazin-6(5*H*)-on showed higher inhibitory activity than the corresponding amino compound. It had increased anti-bacterial activity as well.

It is clear that, to provide a detailed explanation of the varying inhibitory and biological properties of members of this triazine family, crystals of enzyme–inhibitor complexes must be prepared and their crystal structures be solved near atomic resolution. It is well known that the modelling approach with its uncertainties cannot be a substitute for this type of study; after all, it is an assumption that the triazine and the pyrimidine ring of trimethopim will superimpose when members of this triazine family bind to the enzyme, which is the starting point of our modelling efforts. At the moment, we are in the process of trying to prepare single crystals of enzyme members of the triazine family complexes suitable for X-ray crystallographic studies, but so far we have met with limited success.

Based on the evidence accumulated from this study, our future work will be focused on attempts to synthesize and test potential DHFR inhibitors by suitably modifying members of this series.

Experimental protocols

Chemistry

Melting points were determined on a Buchi capillary melting apparatus and are uncorrected. IR spectra were recorded on a Perkin–Elmer 883 spectrophotometer. All compounds gave sharp absorption bands at 3500–3430, 3400–3200 and 1660–1640 cm^{-1}, in agreement with the reported values for diamino-*s*-triazines [24].

^{1}H-NMR spectra were obtained at 200 MHz on a Brucker AC200 instrument using $CDCl_3$ as the solvent and tetramethylsilane as the internal standard. Chemical shifts are reported in δ units (ppm) and coupling constants in Hertz.

UV spectra were obtained on a Perkin–Elmer Lamda7 spectrophotometer. All compounds gave broad absorption bands at 213–215 and 273–283 nm, in agreement with the reported values for UV absorptions for *s*-triazines [25].

Analyses indicated by the symbols of the elements were within ±0.4% of the theoretical values and were carried out at the CNRS, the Central Department for Microanalysis, Vernaison, France.

*Preparation of 2-amino-4-(tricyclo[3.3.1.1^{3,7}]decyl-1)-6-dimethylamino-1,3,5-triazine **1a***

To a solution of 2.98 g (0.018 mol) of freshly prepared base dimethylbiguanide **5** in methanol, 5 ml of sodium methoxide in methanol (freshly prepared from 0.414 g (0.018 mol) of sodium and 15 ml of methanol) followed by 4.35 g (0.021 mol) of adamantane-1-carboxylic acid ethyl ester **6** were added dropwise and the reaction mixture was stirred at 0°C for 30 min. The stirring was continued at room temperature for 2 days and then the reaction mixture was heated to 35°C for 4 days. After cooling, the reaction residue was poured into a 5-fold volume of ice–water. The solid precipitate was filtered off and the mother liquor was extracted several times with diethyl ether. The combined etheral extracts were dried and evaporated under vacuum. The crude liquid residue was washed with anhydrous pentane in order to remove the unreacted ester. The *s*-triazine was immediately crystallized and recrystallized from acetonitrile; mp: 230 ±2°C. ^{1}H-NMR ($CDCl_3$) δ (ppm): 1.74– 2.08(m, 15H, adamantane H), 3.12(s, 6H, $N(CH_3)_2$), 4.87–4.91(br s, 2H, NH_2). IR (nujol) cm^{-1}: ν (NH_2) 3497, 3416, 3220; ν (C=N) 1692. Anal $C_{15}H_{23}N_5$ (C, H, N).

Using the same method, compounds **1b–1f** were synthesized.

*2-Amino-4-(tricyclo[3.3.1.1^{3,7}]decyl-1)-6-piperidino-1,3,5-triazine **1b***

^{1}H-NMR ($CDCl_3$) δ (ppm): 1.5–2.03(m, 15H, adamantane H + 6H, 3,4,5 piperidin H), 3.74–3.81(m, 4H, 2,6 piperidin H), 4.98–5.02(br s, 2H, NH_2). Anal $C_{18}H_{27}N_5$ (C, H, N).

*2-Amino-4-(tricyclo[3.3.1.1^{3,7}]decyl-1)-6-morpholino-1,3,5-triazine **1c***

^{1}H-NMR ($CDCl_3$) δ (ppm): 1.74–2.07(m, 15H, adamantane H), 3.65–3.89(m, 8H, morpholin H), 4.55–4.97(br s, 2H, NH_2). Anal $C_{17}H_{27}N_5O$ (C, H, N).

*2-Amino-4-(tricyclo[3.3.1.1^{3,7}]decyl-1)-6-(4-methyl-piperazino)-1,3,5-triazine **1d***

^{1}H-NMR ($CDCl_3$) δ (ppm): 1.57–2.47(m, 15H, adamantane H), 2.31(s, 3H, CH_3), 2.61(t, 4H, 3,5-piperazine H, A_2X_2, J = 6–7 Hz), 3.75(t, 4H, 2,6 piperazin H, A_2X_2, J = 6.5–7 Hz), 4.93–4.98(br s, 2H, NH_2). Anal $C_{18}H_{28}N_6$ (C, H, N).

*2-Amino-4-(tricyclo[3.3.1.1^{3,7}]decyl-1)-6-cyclohexylamino-1,3,5-triazine **1e***

^{1}H-NMR ($CDCl_3$) δ (ppm): 1.15–1.61(m, 10H, cyclohexylamine H), 1.55–2.03(m, 15H, adamantane H), 3.69–4.18(m, 1H, NH), 4.86–5.01(br s, 2H, NH_2). Anal $C_{19}H_{29}N_5$ (C, H, N).

*2-(Tricyclo[3.3.1.1^{3,7}]decyl-1)-4-dimethylamino-1,3,5-triazine-6(5H)-on **1f***

^{1}H-NMR ($CDCl_3$) δ (ppm): 1.55–2.01(m, 15H, adamantane H), 3.58(s, 6H, $N(CH_3)_2$), 10.1(br s, 1H, NH). Anal $C_{15}H_{22}N_4O$ (C, H, N, O)

Compounds **2a** and **2b** were prepared according to the same protocol, using adamantane acetic acid ethyl ester.

2-Amino-4-(tricyclo[3.3.1.1^{3,7}]decyl-1-methyl)-6-dimethyl-amino-1,3,5-triazine ***2a***
^{1}H-NMR($CDCl_3$) δ (ppm): 1.55–2.01(m, 15H, adamantane H), 2.28(s, 2H, $-CH_2-$), 3.12(s, 6H, $N(CH_3)_2$), 5.05–5.12(br s, 2H, NH_2). Anal $C_{16}H_{25}N_5$ (C, H, N).

2-Amino-4-(tricyclo[3.3.1.1^{3,7}]decyl-1-methyl)-6-cyclohexyl-amino-1,3,5-triazine ***2b***
^{1}H-NMR($CDCl_3$) δ (ppm): 1.1–1.4(m, 10H, adamantane H), 1.54–1.78(m, 12H, (6H adamantane H + 6H cyclohexylamine H)), 1.80–1.89(s, 2H, CH_2), 1.87–2.02(m, 5H, cyclohexylamine H), 4.98–5.11(br s, 2H, NH_2). Anal $C_{20}H_{31}N_5$ (C, H, N).

2-Amino-4-benzylamino-6-(4-t-butyl-phenyl)-1,3,5-triazine ***3a*** *and 2-amino-4-cyclohexylamino-6-(4-t-butyl-phenyl)-1,3,5-triazine* ***3b***
Compounds **3a** and **3b** were prepared as described in [11].

2-Amino-4-benzyl-6-(tricyclo[3.3.1.1^{3,7}]decyl-1-amino)-1,3,5-triazine ***4***
Compound **4** was synthesized according to the same protocol using phenylacetic acid ethyl ester. ^{1}H-NMR ($CDCl_3$) δ (ppm): 1.55–2.12(m, 15H, adamantane H), 2,2(s, 2H, CH_2), 2.8(s, 1H, NH), 5.0(s, 2H, NH_2), 7.02(m, 5H, C_6H_5). Anal $C_{20}H_{25}N_5$ (C, H, N).

Single-crystal X-ray structure analysis

2-Amino-4-(tricyclo[3.3.1.1^{3,7}]decyl-1)-6-morpholino-1,3,5-triazine ($C_{17}H_{25}N_5O_1$) ***1c***
Colorless, needle-shaped crystals were obtained at room temperature by slow evaporation from a methanol solution: triclinic P1: a = 6.901(4), b = 12.876(4), c = 9.321(7) Å; α = 85.33(4), β = 86.49(5), γ = 89.52(4)°; V = 823.94 A^3; Z = 2, D_m = 1.26 Mg•m^{-3}, D_c = 1.27 Mg•m^{-3}; CuK_α λ = 1.5418 Å, μ = 5.79 mm^{-1}, F(000) = 340. Data crystal size 0.1 x 0.25 x 0.6 mm.

Enraf Nonius CAD-4 diffractometer, Ni-filtered CuK_α, moving-crystal/moving counter technique ($2° < 2\theta < 120°$). 61 reflections with $11.9° < \theta < 46.8°$ were used to measure lattice parameters. Index range: h = –7…7, k = –13…0, l = 0…10. Reflection 1 –1 –2 was used as the intensity standard; average count 28488; σ = 317.6.

2294 reflections were measured, 1335 reflections were considered as observed (Rint 0.06%) with $F > 3\sigma(F)$. The intensities were corrected for Lorentz and polarisation effects but not for absorption.

The structure was solved in $P\bar{1}$ by direct methods using SHELXS86 [26]. The E-map from the best solution revealed all non-hydrogen atoms. Hydrogen atoms were either located from difference Fourier syntheses or their positions were calculated. The hydrogen atoms were refined isotropically and the non-hydrogen atoms anisotropically, by full-matrix least-squares calculations utilizing SHELX76 [27]. The refinement converged at R = 0.095, wR = 0.098, w = $(\sigma^{-2}(F) + 0.000632*F^2)^{-1}$.

All calculations were performed on a VAX 3100 computer.

2-Amino-4-(tricyclo[3.3.1.1^{3,7}]decyl-1)-6-cyclohexylamino-1,3,5-triazine ($C_{19}H_{29}N_5$) ***1e***
$C_{19}H_{29}N_5$ + $2CH_3OH$ ($C_{21}H_{37}N_5O_2$) monoclinic $P2_1/c$: a = 6.784(4), b = 21.060(8), c = 15.298(7) Å; α = 90.0, β = 89.11(7), γ = 90.0°; V = 2185.38 A^3; Z = 4, D_m = 1.20 Mg•m^{-3}, D_c = 1.19 Mg•m^{-3}; CuK_α λ = 1.5418 Å, μ = 5.44 mm^{-1}, F(000) = 856.

Needle-shaped, colorless crystals were grown by slow evaporation from methanol at room temperature. Unit cell parameters and space group were determined from precession photographs and improved by least-squares refinement of the setting angles for 12 high angle reflections automatically centred on a Picker Facs-1 diffractometer. The unit cell contains two molecules of methanol per asymmetric unit.

Intensity data were collected at room temperature from a crystal of 0.3 x 0.06 x 0.04 mm using CuK_α radiation (λ = 1.5418 Å) and θ–2θ scan mode. The 2θ range was $3° < 2\theta < 110°$.

A total of 2750 reflections were recorded and 814 were considered observed at the 3σ level ($I > 3\sigma(I)$).

The intensities were corrected for Lorentz and polarization effects but not for absorption.

The structure was solved in $P2_1/c$ by direct methods using SHELXS86 [26]. The E-map from the best solution revealed all non-hydrogen atoms. Hydrogen atoms were either located from difference Fourier synthesis or their positions were calculated. The hydrogen atoms were refined isotropically and the non-hydrogen atoms anisotropically, by full-matrix least-squares calculations using SHELX76 [27]. The refinement converged at R = 0.093 (unit weights). All calculations were performed on a VAX 3100 computer.

Molecular modelling

An Evans and Sutherland PS390 interactive graphics system and a Stardent Titan P1 supermini system were used in the modelling studies. Models for most of the compounds listed in table I have been constructed based on the crystallographically determined structures using the computer program BIOGRAF [28]. The crystal structures determined (see *Results*) correspond to energetically preferred conformations. For compounds with two torsional degrees of freedom in their side chains, several low energy conformations can be adopted.

Enzyme inhibition assay
Compounds were evaluated spectroscopically on a Beckman instrument at 340 nm and 30°C for inhibitory activity against L1210 mouse dihydrofolate reductase. The assays were carried out in 100 mM phosphate buffer (pH 7.9) and 100 mM KCl in the presence of 100 μM NaDPH, 20 μM dihydrofolic acid (prepared according to [29]) and 0.1 units of the enzyme. The compounds were dissolved in 50% ethanol and added to the assay mixture so that a final concentration of up to 50 μM was obtained. At higher concentrations, most of the compounds precipitated. After 5 min of incubation, the reaction was initiated by DHFR [16]. The reaction rates (decrease in absorption) were compared to the rate of the uninhibited reaction measured simultaneously. Each experiment was performed at least in duplicate and the mean values of percentage inhibition are reported (table IV). For compounds **1e**, **2a** and **2b**, the experiments were also performed at different suitable concentrations and I_{50} values were calculated (see *Results*).

Antitumor activity
In vitro testing against murine leukemia P388 (9P5) and KB (9KB5) cells (human rhinopharynx cancer) were conducted according to NCI procedures [17]. *In vitro* cytotoxicity against NSCLCN6 (human bronchopulmonary carcinoma) was assayed, using the following procedure. Tests were carried out in 96-well microplates (Falcon 3072). Each well containing

50 μl of RPMI medium supplemented with 10% fetal bovine serum received 7000 cells. The test solution (50 μl) was added in decreasing concentrations in duplicate. Microtest plates were incubated for 72 h at 37°C in 5% CO_2 in air [18]. Cell proliferation was estimated using a calorimetric method [19].

Microplates were read by a multiscan (Titertek) using a 570-nm filter. The optical density of each well thus enabled the dose–effect curve and the inhibition concentration for 50% of the control cell growth (IC_{50}) to be determined for each compound.

Anti-bacterial and anti-fungal activities

The anti-microbial activity of the compounds was assayed *in vitro* using an agar dilution method against several bacteria and fungi [20, 21].

Bacteria. The following bacteria were utilised: *Staphylococcus aureus* of the laboratory collection, *Streptococcus faecalis* ATCC 10541, *Escherichia coli* CCM 5172, *Proteus mirabilis* CCM 1944 and *Pseudomonas aeruginosa* CCM 1960.

Fungi. Candida albicans CNCM 1180-79, *Aspergillus versicolor* CCM 1187-79, *Cladosporium cladosporoides* CNCM 1185-79 and *Penicillium verucosum* CNCM 1186-79.

The test media were prepared by diluting the test compounds to a concentration of 400–500 μg/ml in Muller–Hinton agar (bacteria) or Sabourand dextrose agar (fungi). Inocula were prepared from 24-h cultures grown in Muller–Hinton broth (bacteria) or Sabourand dextrose broth (fungi). The final suspension in sterile saline contained 10^8 bacteria/ml or 10^5 fungi/ml. Drug-free plates were used as the control of positive growth of the given strains. Benzylpenicillin or miconazole nitrate were used as reference compounds. The test and control plates were inoculated with 0.01 ml of the final suspension and were incubated at 37°C for 18 h (bacteria) or at 30°C until visible growth was evident in the drug-free plates (fungi). The results are expressed as the percentage of growth inhibition.

Anti-viral activity tests

All products were tested against herpes simplex virus (HSVI) and polio I virus (polio) in concentrations < 100 μg/ml. The test method has been described previously [22].

Acknowledgments

The DHFR inhibition assays were carried out in the Astbury Department of Biophysics, University of Leeds, UK. The authors express their thanks and gratitude to AJ Geddes for providing the facilities, equipment and support and for many useful and stimulating discussions.

References

1 Blaney JM, Hansch C, Shipo C, Vittoria A (1984) *Chem Rev* 84, 333–407
2 Modest EJ, Foley GE, Pechet MU, Farber S (1952) *J Am Chem Soc* 74, 855–856
3 Baker BR, Ashton WT (1973) *J Med Chem* 16, 209–214; (1989) *Drugs Future* 14, 138–141
4 Greco WR, Hakala MT (1980) *J Pharmacol Exp Ther* 212, 39–41
5 Antoniadou-Vyzas A, Foscolos GB (1986) *Eur J Med Chem* 21, 73–74
6 Garoufalias S, Vyzas A, Fytas G, Foscolos GB, Chytiroglou A (1988) *Ann Pharm Fr* 46, 97–104
7 Cody V (1984) *Molecular Basis of Cancer. Part B. Macromolecular Recognition, Chemotherapy and Immunology* (Rein R, ed) Alan R Liss, New York, 275–284
8 Cody V (1986) *J Mol Graphics* 4(1), 69–73
9 Shapiro SL, Parrino VA, Freedman L (1959) *J Am Chem Soc* 81, 3728–3736
10 Shapiro SL, Parrino VA, Freedman L (1959) *J Am Chem Soc* 81, 2220–2225
11 Guioca V (1973) *Ann Pharm Fr* 31, 283–292
12 Bergh JJ, Breytenbach JC, Wessels PL (1989) *J Pharm Sci* 78, 348–350
13 Hamodrakas SJ, Hempel A, Camerman N, Offensmeyer FP, Tsitsa P, Antoniadou-Vyzas E, Camerman A (1992) *J Crystallogr Spectrosc Res* 22(5), 607–614
14 Gessmann R, Petratos K, Hamodrakas SJ, Tsitsa P, Antoniadou-Vyzas E (1992) *Acta Crystallogr* C48, 347–350
15 Stammers DK, Champness JN, Beddell CR, Dann JG, Eliopoulos E, Geddes AJ, Ogg D, North ACT (1987) *FEBS Lett* 218, 178–184
16 Thillet J, Absil J, Stone SR, Pictet R (1988) *J Biol Chem* 263, 12500–12508
17 Geran RJ, Greemberg NH, McDonald HM, Schumacher AM, Abbot BJ (1972) *Cancer Chemother Rep* 3, 1–17
18 Roussakis C, Dabuis G, Gratas C, Auduin A (1986) Abstracts of Papers, Vth Symposium NCI EORTC, Amsterdam, 22–24, 412
19 Mosmann T (1983) *J Immunol Methods* 65, 55–63
20 Barry AL (1980) *Procedures for Testing Antimicrobial Agents in Agar Media.* Williams and Wilkins Co, Baltimore, MD
21 Holt RJ (1975) *J Clin Pathol* 28, 767–774
22 Vanden Berghe DA, Vlietinck AJ, Van Hoof L (1986) *Bull Inst Pasteur* 84, 101–147
23 Hithins GH, Burchall JJ (1965) *Adv Enzymol* 27, 417
24 Bellenger P, Hamon M, Mahuzier G (1983) *Ann Pharm Fr* 41, 327–337
25 Alkalay D, Volk J, Bartlett F (1976) *J Pharm Sci* 65, 525–529
26 Sheldrick GM (1985) *Crystallographic Computing 3* (Sheldrick GM, Kruger C, Goddard R, eds) Oxford University Press, 175–189
27 Sheldrick GM (1976) *SHELX76 Program for Crystal Structure Determination.* University of Cambridge, UK
28 Biodesign Inc (1989) *BIOGRAF.* Biodesign Inc
29 Blakley RL (1960) *Nature* 188, 231–232